

Rob Bamber, Christian Colin, Gilles Bignan, Bruce Edwards,  
Christian Gonner, and Chris Waldon

# Conceptual Design of Test Devices for the JHR Tailored to the Needs of the Nuclear Fusion Community

Enquiries about copyright and reproduction should in the first instance be addressed to the Culham Publications Officer, Culham Centre for Fusion Energy (CCFE), K1/083, Culham Science Centre, Abingdon, Oxfordshire, OX14 3DB, UK. The United Kingdom Atomic Energy Authority is the copyright holder.

# Conceptual Design of Test Devices for the JHR Tailored to the Needs of the Nuclear Fusion Community

Rob Bamber<sup>1</sup>; Christian Colin<sup>2</sup>; Gilles Bignan<sup>2</sup>; Bruce Edwards<sup>1</sup>; Christian  
Gonnier<sup>2</sup>; Chris Waldon<sup>1</sup>

<sup>1</sup> *Culham Centre for Fusion Energy, Culham Science Centre, Nr Abingdon, OX14 3DB UK*

<sup>2</sup> *DEN/DER/SRJH, Commissariat à l'énergie atomique et aux énergies alternatives, CEA  
Cadarache, 13108 Cedex St Paul-lez-Durance, France*



# 1 Conceptual Design of Test Devices for 2 the JHR Tailored to the Needs of the 3 Nuclear Fusion Community

---

## 4 **Authors**

5 **Rob Bamber<sup>1</sup> \*; Christian Colin<sup>2</sup>; Gilles Bignan<sup>2</sup>; Bruce Edwards<sup>1</sup>; Christian Gonnier<sup>2</sup>;**  
6 **Chris Waldon<sup>1</sup>**

7 <sup>1</sup> Culham Centre for Fusion Energy, Culham Science Centre, Nr Abingdon, OX14 3DB  
8 United Kingdom

9 <sup>2</sup> DEN/DER/SRJH, Commissariat à l'énergie atomique et aux énergies alternatives, CEA  
10 Cadarache, 13108 Cedex St Paul-lez-Durance, France

11 \* Corresponding author: rob.bamber@ukaea.uk

12

1 **Abstract**

2 Since 2015, within the scope of the Jules Horowitz Reactor (JHR) project a  
3 collaborative effort between CCFE in the UK and CEA in France has sought to develop test  
4 devices for the JHR suitable for the needs of fusion researchers. It is hoped that in having  
5 optimized experimental devices designed will facilitate use of the JHR by the fusion  
6 community.

7 The project chose to focus on more instrumented test devices as it was felt that post-  
8 irradiation examination (PIE) type experiments at conventional temperatures could be  
9 undertaken with limited modifications to existing test devices. After internal exploration of the  
10 options, three potential test devices were identified; i) testing of ceramic functional materials;  
11 ii) testing at cryogenic temperatures; and iii) testing of thermo-mechanical fatigue. Each of  
12 these devices has been conceptually designed, demonstrating feasibility.

13 This paper describes each of the conceptual designs at their current level of maturity.  
14 Future collaborative work planned between the two parties will aim to develop these devices  
15 further.

16 **Keywords**

17 JULES HOROWITZ REACTOR; TEST DEVICE; FUSION MATERIAL NEEDS

## 1 I. Introduction

2 The Jules Horowitz Reactor (JHR) is a 100MW<sub>th</sub> tank in pool type material research  
3 reactor (MTR) and is currently under construction at CEA Cadarache in southern France.  
4 The JHR is expected to commence operation at the end of the current decade as part of the  
5 replacement for the aging fleet of European MTRs. The JHR will support materials research  
6 for both the current fleet (generation II and III) and advanced (generation IV) fission reactors  
7 in addition to providing isotopes for medical use (e.g. <sup>99</sup>Mo) [1].

8 The magnetic confinement nuclear fusion program is entering into an interesting  
9 transition, the development of ITER in particular demonstrates the progression from  
10 experimental physics devices into technological prototypes [2]. In addition to the ITER  
11 project, most of the partner organizations are developing conceptual designs for a prototype  
12 power plant, often named DEMO [3]. As these devices become larger and more expensive,  
13 higher reliability and better quality material data is required. In addition to this, the  
14 combination of high heat fluxes, high quality vacuum and irradiation damage found in the  
15 fusion environment often provides unique design and material challenges.

16 A collaborative project has been launched between CCFE and CEA in order to  
17 examine the need and develop experimental devices for the JHR which would facilitate its  
18 ability to aid in resolving the fusion community's upcoming material science challenges.

## 19 II. Design Philosophy

20 Typically a material development program is split into three parts [4];

21 **The Selection Phase:** where many material options are tested in a cost  
22 effective manner to determine the most promising options. In order to contain costs  
23 and maximize the number of samples available in testing, these investigations  
24 typically involve post-irradiation examination (PIE) only and minimize the  
25 instrumentation available.

26 **The Characterization Phase:** After materials have been down selected,  
27 further investigation is undertaken in order to create a database of material  
28 performance. The goal at this stage is to provide models and laws describing their  
29 behavior. At this stage, it is also useful to determine whether synergistic effects which  
30 may be missed by PIE are of concern. This typically leads to test devices with more  
31 instrumentation and better environmental control (thermal, chemical, mechanical  
32 loads) than those used in the selection phase. Consequently, costs per specimen  
33 increase as the program develops.

34 **The Qualification Phase:** Before a material can be accepted into commercial  
35 service, the database created in the characterization phase will need to be made  
36 more robust. The data produced here include both normal and off-normal (up to  
37 accidental) operating conditions. These types of study are likely to include long-term  
38 aging effects and significant numbers of samples to provide values of a given  
39 statistical certainty.

40 It is felt that different parts of the fusion program are at different stages in this path,  
41 for example the DEMO programs are predominantly at the material selection stage, whereas  
42 ITER is somewhere around the characterization or even the qualification phase.

43 Considering the timescales for JHR operation and the likely progress of the DEMO  
44 program before then, it was decided to concentrate this work on test devices capable of the  
45 latter phases described above. This implies test devices capable of online testing and higher  
46 instrumentation of samples at the expense of sample quantities. This approach was further

1 justified by the fact that both the MICA and OCCITANE test devices in the JHR cater for PIE  
2 type experiments (albeit with certain temperature limitations) [4].

### 3 **III. FUSERO A – Ceramic Functional Materials Testing**

4 It is clear that ceramic functional materials will be required in both diagnostic and  
5 plasma resonance heating systems, providing both vacuum and radioactive inventory  
6 confinement [5]. In order to successfully design these components some knowledge of the  
7 evolution of their structural and functional characteristics with irradiation must be known. This  
8 design is intended to facilitate the generation of data in support of this study.

9 The functional properties of interest include electrical properties for the heating  
10 systems and optical properties for diagnostic windows. In addition to this, sub-critical crack  
11 growth (SCCG) can play a large part in limiting the lifetime of ceramic components [6] and  
12 therefore designs for online testing of these parameters will also be investigated.

13 This test device is intended to be utilized in the reflector area of the JHR.

#### 14 **III.A. Existing Concepts**

##### 15 **Electrical Properties**

16 The electrical properties of interest include direct current resistivity and electrical  
17 impedance at both ~50MHz and ~170GHz, the resonant frequency of the ions and electrons  
18 which constitute the plasma respectively [7].

19 Several DC resistivity measurement test devices have been successfully used in  
20 other MTRs. An example of a particularly advanced type which could apply an electrical field  
21 to the ceramic during the irradiation was developed for the High Flux Reactor at Oak Ridge  
22 National Lab [8].

23 One high frequency online test device was found in the literature [9], the device was  
24 used on a TRIGA type pulsed reactor in order to measure prompt effects. This device is  
25 capable of determining the electrical properties of ceramic materials at around 50MHz.

26 No existing designs were found for online testing at the higher frequencies suitable for  
27 electron resonance. Indeed, testing at these frequencies either requires an unfeasibly large  
28 amount of space in the free space method or impossibly small test samples via a resonance  
29 method.

##### 30 **Optical Properties**

31 No devices were found in the literature currently capable of determining the optical  
32 properties of ceramic materials (e.g. fused silica) during the irradiation.

##### 33 **SCCG Properties**

34 Although no device is currently available for determination of alumina's SCCG  
35 properties during neutron irradiation, Pells and Boothby [10] undertook this experiment whilst  
36 exposing samples to gamma irradiation from a Cobalt-60 source.

#### 37 **III.B. Testing Envisaged**

38 Based upon the existing options for electrical testing, this work decided to focus on  
39 designing a test device suited for diagnostic windows. The device will measure the evolution  
40 of both the functional (optical) properties in addition to the SCCG parameters necessary to  
41 enable the construction of a robust structural justification for the ceramic material.

42 The optical testing will be performed by passing a beam of light of known wavelength  
43 through the ceramic sample. A detector will then measure the beam, allowing for any



1 degradation of the optical properties to be determined. Periodically, the beam will reach the  
2 detector without traversing any samples, this will allow for any degradation of the  
3 experimental equipment to be understood.

4 The SCCG testing will involve the biaxial loading of disc samples (loading axis  
5 perpendicular to the disc plane), whilst measuring the time to failure of the sample. By  
6 varying either the stress or the stressing rate, the parameters describing the crack growth  
7 law can be deduced [11].

### 8 III.C. Design Overview

9 The sample holder is split into three sections, there are the optical specimens  
10 themselves, situated near the maximum flux plane (PFM), above them are six levels of  
11 actively loaded mechanical samples whilst below there is unutilized space, which could be  
12 filled with PIE samples.

13 It should be noted that the ratio of gamma to neutron irradiation is an important  
14 parameter for ceramic materials [11], probably due to the non-metallic nature of their  
15 bonding. The ratio of gamma to neutron irradiation in a fission type reactor is far higher than  
16 that of a fusion device<sup>1</sup> and therefore a tungsten shield is included in the design to reduce  
17 this gamma dose to levels more consistent with fusion environments.

18 The tungsten shield is incorporated into a modified cooling tube in order to interface  
19 with the JHR's reflector structure. As the tungsten material is expensive, it is proposed that  
20 the cooling tube designed for the cryogenic test device with its 18mm thick tungsten screen  
21 (see §IV), could be incorporated into this device. An optimisation study of this tungsten  
22 screen will be required to verify that in addition to respecting the safety criteria, it will serve  
23 both purposes well.

24 The test device itself is foreseen to be a fairly simple 2 mm thick stainless steel shell  
25 and so shall not be detailed here, with only the paniers of the sample holder described in  
26 detail.

27 An overview of the device is shown in Figure 1, where it can be seen that there is an  
28 annular gap of 3mm around the periphery of the sample holder/paniers annotated "Heater  
29 Location". This is in order to install the electrical heating system currently under development  
30 for the MICA experimental device, which will allow temperature control in up to six axial  
31 stages. Between this heating system and the device shell itself there will be a gas gap of  
32 some tens of microns to set the approximate temperature of the samples.

### 33 Optical Equipment

34 Fiber optics are the most convenient way to transmit light between the optical  
35 equipment in the I&C room and the samples in the reactor pool, however it is not evident that  
36 their performance in a high radiation field will be acceptable, see for example [12]. Therefore  
37 fiber optic wires will be used to transfer the light from the I&C cubicle to the top of the sample  
38 holder where a collimator will transform it into a light beam of approximately Ø6mm to  
39 traverse the high radiation field adjacent to the core. Here the beam will pass through one of  
40 the samples before continuing down to the very bottom of the test device (to minimize the  
41 radiation load on these optical components) before being collected in a collimator, turned  
42 through 180° in a fiber optic cable and re-made into a beam to ascend through the center of

---

<sup>1</sup> The ITER windows are anticipated to receive  $9\text{E}^{10}\text{n/cm}^2\text{s}$  and  $350\text{Gy/hr}$  [12]. Position C311 of the JHR reflector (will be used for PROSPERO but is representative of a reflector position) is anticipated to provide an irradiation of  $3.1\text{E}^{14}\text{n/cm}^2\text{s}$  and  $9\text{E}^6\text{Gy/hr}$ . This gives a ratio of neutron to gamma irradiation approximately 7.5 times lower.

1 the test device. Alternatively if subsequent R&D finds that fiber optic cables are inadequate,  
2 mirrors could be employed in the base of the device.

3 One major inconvenience of the fiber optical system is that collimators are sized for a  
4 given wavelength, the range currently considered have standard components approximately  
5 every 150nm between 400 and 2000nm. Therefore although, the wavelength cannot be  
6 swept during the irradiation, for each experiment the device could be set for an optimum  
7 wavelength (within these bounds) as the design allows for easy changes between different  
8 collimators.

9 There are three levels of optical samples, with each level containing seven samples  
10 and a free space. The panier of each level is able to rotate around the axis of the test device,  
11 independently of the paniers on other levels. The free space is positioned in the beam-line  
12 when testing samples on one of the other levels.

13 As shown in Figure 2, each (identical) panier contains seven samples (21 in total), of  
14  $\text{\O}12\text{mm} \times 6\text{mm}$  thick discs. The paniers are rotated by three concentric shafts, which run  
15 around the outside of a tube which in turn protects the central beam line. The shafts have  
16 splines at either end in order to interface with the paniers and gearbox. Above the splines, in  
17 the head of the device, a gearbox interfaces between the shaft described above and a  
18 flexible drive, connecting to a stepper motor in the I&C cubicle.

19 Each panier will contain several dosimeter wires and a thermocouple to aid in  
20 temperature regulation. The panier will be prevented from rotating more than  $360^\circ$  in order to  
21 allow the thermocouple cable to transmit signals to the I&C cubicle. A light source and  
22 detector will be installed in the I&C cubicle, these will be connected to the fiber optics used to  
23 transmit the light signals to and from the reactor pool.

## 24 **Mechanical Equipment**

25 The mechanical equipment is designed predominantly to round out the long-term  
26 strength data for ceramics with additional in-situ testing in a radiation environment. There are  
27 six similar paniers with six samples in each panier (36 concurrent samples).

28 The device is designed to be able to bi-axially load the ceramic discs with up to  
29 100MPa (typically diagnostic window materials see some 10's of MPa from the pressure  
30 load) and record the time to failure. As with the optical stages, the electrical heating is  
31 provided on the exterior of these paniers and their temperature controlled with the aid of  
32 thermocouples in the structure.

33 Although the European standard [13] for this testing advocates the use of uniaxial  
34 testing, the biaxial bend testing is preferred due to its compact specimen size and similarity  
35 to the in-service stress state for ceramic windows on fusion devices (as pressure retaining).  
36 Mimicking the in-service stress state of components facilitates interpretation of the results.

37 The panier is annular in form and fits around the outside of the drive shafts of the  
38 optical paniers, as shown in Figure 3. The paniers are mounted upside down as the  
39 connections to the uppermost panier then do not need to traverse it and the effect of gravity  
40 upon the testing is negligible. The panier is assembled from a subassembly which includes  
41 the body, bellows and contactor assemblies. The samples and dosimeters are then added to  
42 this subassembly before the lid is attached by seven M4 screws.

43 Each panier holds six samples, these are 1mm thick discs of  $\text{\O}10\text{mm}$ . Although this  
44 thickness is not representative of the ITER windows (6mm to 12mm dependent upon  
45 diameter [11]), it is unfeasible to provide the force required to adequately stress significantly  
46 thicker samples. It is thought that if the samples are taken from a representative block this  
47 technique will give adequate results [13]. The dependence of ceramic performance on

1 surface finish is well known and it is recommended that experimenters use the same  
2 manufacturing techniques between samples and eventual components in order to correctly  
3 replicate the flaw distribution and surface finish.

4 The samples are held in biaxial bending with the bellows assembly applying a load to  
5 a ring of Ø8mm on one side of the ceramic disc. The lid provides the reaction force to this  
6 load on a circle of Ø3.2mm. Calculation after [14, p. 487] has shown that a force of 141N will  
7 provide a stress of 100MPa with 2.5µm of deflection (assuming an elastic modulus of  
8 350GPa for alumina). This deflection value will not be measured as this device is more  
9 interested in the time to failure of samples, in order to determine the SCCG parameters.

10 The bellows assemblies are common for all samples and are based upon dimensions  
11 of a standard hydro-formed bellows from a commercial catalogue. A stop is provided after  
12 ~0.25mm of travel (to be compared to the expected deflection prior to sample failure of  
13 2.5µm) to prevent damage to the bellows. Calculation shows that the bellows can provide  
14 150N of force with an internal pressure of 50bar, inducing a hoop stress of around 250MPa  
15 in the bellows. The gap between the head of the bellows and the body should be sized  
16 during the preliminary design phase to allow free and clear movement of the head whilst  
17 maintaining a good heat transfer between the two.

18 There are two gas ports on the base where the tubes of Ø1.6mm are welded (1/16").  
19 The two ports are supplied on each bellows in order to daisy-chain all of them in a single  
20 panier together. Obviously this limits the applied force to each specimen as being identical  
21 but this is not thought to be an issue as with ceramics many repetitions of a test will be  
22 required due to the statistical nature of ceramic strength.

23 During commissioning, a pressure force curve for each bellows will be measured and  
24 used to control the loading of the samples.

25 The lid is held in place by seven M4 screws. Calculations show that with a core  
26 diameter of 3.14mm, the nominal tensile stress from the bellows loading in each screw is  
27 around 20MPa.

28 An instrumentation system is required in order to determine the time of fracture of  
29 each sample. Two options are currently being considered, one involving seven wires and one  
30 involving two wires. In the former system each sample has a connection that will be made  
31 upon failure (incorporated into the bellows stops) with a common return. The latter system  
32 places each connection switch in series with a high resistance (~50Ω) object. These are then  
33 connected in parallel and the changing resistance of the total circuit used to infer the number  
34 of samples broken in each panier. Figure 4 shows a schematic of this system. Although the  
35 latter system is unable to determine which sample broke, this is unimportant information as  
36 they are in nominally identical conditions.

#### 37 **IV.FUSERO B – Cryogenic Testing**

38 In order for a future fusion reactor to supply more energy than it consumes at least  
39 part of the magnetic field will need to be supplied via super-conducting magnets. The  
40 performance of these magnets and their evolution under irradiation, both neutrons and  
41 gammas, requires evaluation. Both the conducting and insulating material will need to be  
42 studied in a suitable environment. Due to the large forces exerted on the fusion magnet  
43 system during a plasma disruption, in addition to the electrical and thermal properties, the  
44 evolution of structural properties are required for adequate design of a magnet system. The  
45 literature surveyed doesn't discuss the possibility of prompt effects calling for in-situ testing.  
46 Therefore for the purpose of this irradiation device, it has been assumed that PIE is adequate

1 for assessing the damage to superconducting components and that online measurement of  
2 properties is not required.

3 In addition to this, the materials modelling community have a desire to validate their  
4 primary damage models (i.e. models which don't include recombination effects). A cryogenic  
5 facility would be able to "freeze in" many of these defects allowing examination of nearly the  
6 primary damage.

7 Both of these objectives require a test device design which could cool materials to  
8 cryogenic temperatures during the irradiation. Additionally post irradiation some samples  
9 may need to be kept at cryogenic temperatures until testing was complete, as the JHR will  
10 not include cryogenic hot cell facilities this would include developing a storage and transport  
11 plan.

12 It should be noted that the largest issue with the design of this device is that both a  
13 client and a PIE partner with the ability to test radioactive materials in cryogenic conditions  
14 are yet to be found.

#### 15 **IV.A. Existing Concepts**

16 The literature surveyed has shown that two MTRs have or have had cryogenic testing  
17 capabilities.

18 The now decommissioned Plum Brook reactor, operated by NASA in the US had  
19 cryogenic facilities able to perform irradiations at around 28K (-400°F). Facilities at Plum  
20 Brook included an insertion device into one of the horizontal beam lines. It appears that the  
21 device was regenerating cryogenics but it must be noted that only very limited information on  
22 the operation of this device has been found.

23 The IVV-2M reactor in Ekaterinburg in Russia is also capable of irradiations at  
24 cryogenic temperatures and has performed work for CERN. Very limited detail has been  
25 found regarding the working of this system but it appears that the cryogenic system again  
26 uses a tube location. It appears that small samples can be tested to liquid helium  
27 temperature whilst mechanical specimens can be tested at around 80K [15]. One imagines  
28 the system is technically similar to that utilized by Plum Brook.

#### 29 **IV.B. Testing Envisaged**

30 It is believed that the evolution of the electrical and structural properties of  
31 superconducting magnet materials (conductors, insulators and any structures) under neutron  
32 irradiation will need to be understood before these can be applied in a large, licensed and  
33 commercial fusion device. It is known that higher temperatures can anneal out irradiation  
34 damage of materials and therefore that experiments performed on irradiated materials at  
35 temperatures significantly higher than the operating temperature can provide optimistic  
36 results. Therefore a multipurpose system is proposed that can irradiate and store post-  
37 irradiation various specimens of material at cryogenic temperatures (target of 50K).

38 The large number of properties that require testing, means that a generic device  
39 catering for PIE is the only currently feasible option.

40 In addition to this smaller samples may be used with electron microscopy by the  
41 materials modelling community in order to validate and develop their models.

#### 42 **IV.C. Design Overview**

43 One large technical constraint encountered in this work was the desire to maintain the  
44 cryogenics in the gaseous state. This is to prevent any leakage of cryogenics into the reactor  
45 pool then expanding to many times its initial volume. However, it must be noted that using a

1 gaseous medium degrades performance (i.e. sample temperatures) due to the lower heat  
2 transfer capability than via liquid cryogenes.

3 This design is intended to give the maximum flexibility to users with a panier system.  
4 The paniers can be re-designed and manufactured for a specific experiment at minimal cost,  
5 allowing for different types of sample (e.g. tensile, CT etc.) to be tested as desired by the  
6 user.

7 The major challenge in this design is minimizing the cooling power required as this is  
8 extremely expensive to provide. The laws of thermodynamics mean that at least 15 times the  
9 cooling power is required as electrical power to achieve coolant temperatures of around 20K.  
10 Moreover, the achieved efficiencies of cryogenic plant are often far from ideal and factors  
11 between the cooling power and electrical power of 100 are not uncommon. This necessitates  
12 minimizing the heat leak where possible, although compromises have been made in certain  
13 areas, and minimizing the nuclear heating via the inclusion of a Tungsten shield.

14 Although the project has created a bespoke design for the sample holder and test  
15 device, parts of the system external to the reactor pool (e.g. refrigeration unit, transfer lines  
16 etc.) will be constructed from commercial items.

17 In the design of this device, there are four key design compromises:

- 18 • Maximizing the insulation to minimize heat leak whilst maximizing the  
19 sample volume and simultaneously maintaining ease of assembly,  
20 adequate instrumentation and respecting the packaging limits.
- 21 • Minimizing the gamma dose by adding a tungsten shield whilst  
22 maintaining adequate space for the device.
- 23 • Allowing adequate instrumentation whilst enabling the paniers to be  
24 removed from the test device under cryogenic conditions.
- 25 • Providing adequate positional support to the cryogenic components  
26 whilst minimizing the heat leaks.

27 A CATIA model has been produced of the conceptual design of this device and is  
28 shown in Figure 5. It can be seen that there are three main parts to the in-pool part of this  
29 test device; i) the cooling tube; ii) the test device; and iii) the sample holder. The concept of  
30 the design is such that the cooling tube is modified to include the gamma heating shield,  
31 whilst the test device shell contains the insulating vacuum and the sample holder is the only  
32 part operating at cryogenic temperatures.

### 33 **Cooling Tube**

34 The standard cooling tube is modified by cutting and welding to include a section with  
35 a tungsten shield 18mm thick. The thickness of the tungsten screen is a compromise:  
36 increasing it decreases the cryogenic heat load by reducing the gamma radiation but at the  
37 expense of reducing the space available for the samples and increasing the overall test  
38 device mass.

39 Including the tungsten screen on this tube unfortunately means that this becomes a  
40 bespoke component, although shared with the ceramic functional material test device.  
41 However this arrangement simplifies the design as the tungsten shield requires cooling from  
42 both the inner and outer diameters, this negates the need for an additional cooling channel,  
43 maximizing the flow velocity and therefore the heat transfer in addition to maximizing the  
44 space available for samples.

45 Due to the differential thermal expansion of the tungsten (~4ppm/°C) and the  
46 stainless steel (~16ppm/°C) cladding, it is prudent to use the tungsten in the form of either

1 powder or balls to negate this problem. However this will entail a packing efficiency of  
2 approximately 75%. The impact of this on the thermal conductivity is limited as the wall  
3 boiling criteria are more stringent than the tungsten thermal criteria. A gas gap is included  
4 above the tungsten screen, this is to enable closure of the weld without powder behind it and  
5 any outgassing from interaction between the tungsten and the irradiating media, although  
6 this is thought to be unlikely.

7 The cooling tube includes an orifice to enable the pressure drop of the device to be  
8 adjusted in line with the wider reactor hydraulic design.

9 A simple calculation based upon half-value layers anticipates that this shield will cut  
10 the nuclear heat load by 50%, this assumption will need to be checked via explicit calculation  
11 as the energy levels of gamma are currently unknown in this location.

12 Simple thermo-hydraulic calculations have been performed on the tungsten shield  
13 and large margins are anticipated to both the materials' operating limits and to prevent  
14 boiling in the fluid.

### 15 **Test Device**

16 The test device is a hollow shell in the region of the core and contains the thermally  
17 insulating vacuum. On the outside of this envelope is reflector cooling water at approximately  
18 40°C and at the inside is the vacuum, isolating the cryogenic components. The test device  
19 itself is around ambient temperature (slightly above due to nuclear heating). The device is  
20 centered in the cooling tube by a system similar to utilized elsewhere in the JHR. In fact, the  
21 only difference is that it occurs on reduced diameters in the tungsten screen. The test device  
22 can be considered as four discrete sections, welded together.

23 After advice from an expert in cryogenics, it was determined that it is necessary to  
24 have a secondary vacuum with an ultimate pressure of at most  $10^{-4}$ mbar in order to minimize  
25 the heat leak from the reactor pool. A small turbo-molecular pump is attached to the head of  
26 the test device with a pumping speed of 65l/s. The conductance of the long annular space is  
27 estimated as 12.2l/s, giving an effective pumping speed of 10.5l/s. Using approximations of  
28 the wall gas load and seepage from the joint to the sample holder allows an estimate of the  
29 ultimate pressure of  $10^{-5}$ mbar to be produced.

30 The foot of the device is machined from solid and welded to the tubular "reduced  
31 section" via a butt weld. The geometry (radius and angle) is taken from that of the standard  
32 test device.

33 The reduced section is provided to enter the tungsten shield and includes the conical  
34 piece to join to the standard section above. It is simply a tube with dimensions OD 61mm, ID  
35 57mm.

36 The standard cylindrical section includes the interface with the cooling tube and is  
37 standard to the JHR design.

38 The upper section includes the oblong flange for the interface to the sample holder.  
39 The vacuum is increased into an oblong shape to allow the annular cryogen flow and return  
40 arrangement of the sample holder to be separated into two discrete lines for the flow and  
41 return. And more, there is space allocated for both an on-axis port for removal of the paniers  
42 under cryogenic conditions and a feed-through for the thermocouples

43 The wall of the oblong shape is 17.5mm thick at its thinnest point, this is thought to be  
44 sufficient to prevent excessive stress from the vacuum containment. The upper also includes  
45 a small enclosure covered by a 2mm thick steel plate, this will be open to ambient air and will  
46 house the vacuum system equipment. A hollow section along one end offers a protected

1 zone for the access for the control cabling of the vacuum equipment and the rough pumping  
2 line.

### 3 **Sample Holder**

4 The sample holder (see Figure 6) itself is used as the boundary between the  
5 insulating vacuum and the cryogenics as it is important to minimize the mass at low  
6 temperature (to minimize the nuclear heat deposition and therefore the cryogenic heat  
7 loads).

8 The sample holder is predominantly two concentric tubes, featuring a core flow area  
9 and an annular space in which the coolant flows and is returned. At the head of the device,  
10 the concentric tubes of the sample holder are split into four routes, the flow and return lines  
11 and an instrumentation stub all separating from the stub for the on-axis port for the paniers.  
12 The flow and return lines are equipped with commercially available bayonet connections.

13 The sample holder has three centering devices along its length. The lower centering  
14 device is located on a shaft, increasing the conduction path length. Although the other  
15 centering devices are unconventional for cryogenic service and produce relatively large heat  
16 leaks, the need to locate the sample holder well in the event of seismic activity dominates.

17 The sample holder is designed such that the loading can be performed in hot cell  
18 conditions with the sample holder remaining in the vertical position. This is achieved by  
19 unscrewing a plug connection on the on-axis port and placing the paniers in through a check  
20 type valve. Apart from this port the sample holder boundary is completely welded in order to  
21 minimize any leak of cryogenics. This port, particularly the check valve type flap, will require  
22 further development and prototyping.

23 The sample holder itself is left as a hollow tube to allow the maximum flexibility to this  
24 device. This means that future experimenters are entitled to develop their own panier  
25 systems to accommodate any and all sample types that they may wish to test. The cylindrical  
26 cavity held at cryogenic conditions available has dimensions of  $\text{Ø}26\text{mm} \times 600\text{mm}$ . This cavity  
27 is thermally designed to contain up to 1.25kg of material (~50% volume if stainless steel is  
28 used).

29 The number of thermocouples or other instrumentation is a compromise between the  
30 space available for the feedthrough and the cables descending which are in the cryogenic  
31 gas return flow (raising the pressure drop) and the need for accurate temperature  
32 measurement. The basic scheme is such that the 16 thermocouples (two thermocouples  
33 every 75mm of height) are fed through in the top of the sample holder. A dead leg provides  
34 the thermal gradient allowing for this feed-through to be at ambient temperature.

### 35 **Ex-Pool Equipment**

36 External to the in-pool equipment; transfer lines, a roughing vacuum system and a  
37 refrigeration system will need to be provided. The transfer lines and roughing vacuum system  
38 are commercially available items. Although fixed lines are preferable to flexible lines from  
39 both a thermal loss and pressure drop perspective, flexible lines have been retained in this  
40 design due to the need to maintain flexibility in the reactor pool and surrounding area to  
41 facilitate installation and handling of other test devices around the reactor.

42 The refrigeration unit is a bespoke unit. Calculation has shown that the refrigeration  
43 system should be designed to cope with a heat load of 1.25kW, providing 5m<sup>3</sup>/hr of helium  
44 gas at 20K. Both Air-Liquide and Linde-Kryotechnik have supplied similar systems for similar  
45 duties previously.

#### IV.D. Thermal Aspects

A sensibility analysis was undertaken, determining the pressure drop for system pressures between 0 and 10bar gauge. Figure 7 shows that the required pressure drop decreases as the operating pressure is raised, due to the improved heat transfer requiring a lower flow rate. However this process is not linear and therefore a 4 barg operating pressure is proposed. Figure 7 also shows the required flow rate to cool the samples and the heat exchanged between the flow and return legs of the device (see below).

Initial thermal calculations were undertaken which show that a flow rate of 5m<sup>3</sup>/hr appears to be a reasonable design compromise, allowing a bulk fluid temperature rise of around 20K in the circuit and sample temperatures of 46.5K and 61.5K for the Ø4 mm tensile samples and the rectangular samples (Charpy and CT). Although this is in excess of the target temperature of 50K, sub-sized specimens (53.2K at 7.5mm thickness and 46.2K for 5mm thickness) or moving away from the PFM would allow the target temperature to be reached. The dependence of sample temperature upon flow rate is shown in Figure 8.

A pressure drop of 160mbar is estimated for the device, the pressure drop contributions are shown in Table I. It can be seen that the high velocities (necessary for good heat transfer) in the panier region make this the largest contributor to pressure drop.

Table I, estimation of pressure drops

Section	Velocity [m/s]	Reynolds #	$\xi$	$\Delta P$ [mbar]
Flexible Lines	5.75	171000	54	71
Bayonets	Considered negligible			
Inner Pipework	2.7	117000	4	1
Paniers	8.5	28500	29	84
Return	2.7	N/A	1.5	0.5
Return Pipework	2.9	71000	8.2	3
<b>Total</b>				<b>160</b>

The heat loads on the cryogenic system have been estimated. The heat leak through the centering devices was estimated via finite element calculation. Other heat leaks estimated include both the conductive and radiative terms through the insulating vacuum. A summary of the heat loads can be found in Table II, where it can be seen that the major heat leak (greater than <sup>2</sup>/<sub>3</sub>) is the nuclear heat load.

Table II, estimation of cryogenic heat loads

Component	Heat Load [W]
Nuclear Heating	695
Through Insulating Vacuum	50
Bayonet Connections	6
Pumping Power	45
Flexible Pipes	55
Centring Rings	122
Instrumentation Tube	2



On-axis Port	11
<b>Total</b>	<b>986</b>

1  
2  
3  
4  
5  
6  
7  
8  
9  
10  
11  
12  
13  
14  
15  
16  
17  
18  
19  
20  
21  
22  
23  
24  
25  
26  
27  
28  
29  
30  
31  
32  
33  
34  
35  
36  
37  
38  
39  
40  
41  
42  
43

There is a risk of ice forming and either disrupting the correct cooling water flow around the device or damaging the structure due to its expansion upon solidification. In order to quantify this risk, the middle centering ring is deemed the most critical.

A finite element analysis has been undertaken and predicts a heat leak of 40W for the central ring with a minimum value of the fluid wall temperature of 22°C, showing that the risk of freezing is controlled.

Considering the bayonet connections, the KF type flange has a surface (both sides of the connection of 5668mm<sup>2</sup>, if it assumed that the whole heat leak of 3.25W is through this surface, a heat flux of 575W/m<sup>2</sup> is estimated. Typically free convection in water has a heat transfer coefficient of 100W/m<sup>2</sup>K. Using the relation that temperature gradient is equal to the heat flux divided by the heat transfer coefficient a temperature difference of 5°C can be anticipated in the reactor pool. This must be checked during the subsequent design stages and if necessary a protected zone similar to that for the vacuum equipment could be included around the bayonets.

Although the annular tube shape saves a significant amount of space, allowing maximization of the insulating vacuum thickness and sample volumes whilst minimizing the pressure drop, it allows a heat transfer between the flow and return of the cryogenic helium. Utilizing the ε-NTU method of calculating heat exchanger performance, estimates a total heat exchange of 513W (ΔT = ~8.5K). Therefore the fluid entering the panier section will be at 30K as opposed to the 20K delivered by the refrigeration system.

**V. FUSRO C – Thermo-Mechanical Fatigue Testing**

Thermo-mechanical fatigue testing involves the cycling of both mechanical strain and thermal strain onto material specimens in a pre-determined pattern (with the possibility of the thermal and mechanical strains being out of phase). It is currently believed that thermo-mechanical fatigue testing can better predict the fatigue life of components subjected to a changing temperature field than the more traditional strain-life approach.

Many fusion components from breeding blankets to divertor tiles are subjected to a time-varying heat load and so significant benefit could be found from this type of experiment.

There are recognized national and international standards for thermo-mechanical fatigue testing, for example BS ISO 12111:2011, which use tensile specimens on a strain-controlled hydraulic testing machine with a furnace or induction heating system controlling the temperature of the sample. The samples are often hollow to minimize thermal gradients, especially during a temperature transient.

Two sample holders have been conceptually designed to be used in one of the test positions available in the center of a fuel element of the JHR core, this position should maximize the dose rate for the samples. One of the sample holders is for a tensile test device, whilst the other is for a 4-point bending device type specimen. After initial design work, a third alternative performing bi-axial testing on discs loading them similar to Belleville washers was rejected due to the strong spatial variation in mechanical stress gradients and packaging issues. Presently the bending specimen design is preferred with the tensile specimen design kept in reserve pending the results of an initial study to determine the possibility of interpreting the data from a bending-type specimen.

## 1           **V.A.       Existing Designs**

2           At Petten, NRG have developed a test device called POSITIFE to thermally cycle  
3 prototype first wall components. Although this device doesn't cycle mechanical stress, the  
4 thermal stresses are cycled in-phase with an irradiation dose cycling [16]. The whole  
5 prototype is mounted into the reactor pool and its position moved relative to the reactor in  
6 order to cycle the temperature via adjustment of the nuclear heat load.

7           External to the world of MTRs, various alternative methods have been used for  
8 putting fatigue loads onto samples, for example, ultra-sonic methods for high cycle fatigue  
9 [17] or a rotating specimen past a hot and cold source for thermal fatigue [18].

10          It should be noted that the typical schemes for temperature control utilized in MTRs  
11 are not available for this design for the following reasons;

- 12           • As the device is mounted in the center of a fuel element in order to achieve  
13 large damage rates, it is impossible to withdraw it in order to reduce the  
14 nuclear heat load and therefore its temperature.
- 15           • The high temperature difference between the hot and cold extremities of the  
16 cycle make electrical heating unfeasible. This is due to the low thermal  
17 resistance necessary to achieve the low temperature end of the cycle with a  
18 high nuclear heat load necessitating an unfeasibly high electrical heat load to  
19 raise the temperature to the upper temperature range.
- 20           • The mixing of gasses limits the temperature range based upon the ratio of the  
21 thermal conductivities of the mixed gasses.

## 22           **V.B.       Testing Envisaged**

23          This device will cycle material specimens in 4-point bending in purely elastic materials  
24 a 250MPa load can be applied at the surface in the form of both tensile and compressive  
25 stresses. The device will also be able to cycle the sample temperature from approximately  
26 150 to 600°C, over a timescale of around 3 minutes. Both these cycles are to be controlled to  
27 a pre-programmed cycle and may be either in or out of phase.

28          The applied bending moment and surface strain will be measured allowing for  
29 hysteresis loops to be created for various materials.

## 30           **V.C.       Design Overview**

31          The conceptual design of the sample holder is shown in Figure 9 and has a repeating  
32 section for the three samples. One major downside of the 4-point bending approach is that it  
33 is bending moment which is the controlled variable and neither strain nor stress is controlled  
34 directly.

35          The 4-point bending sample is a dog bone type shape with pinned holes locating the  
36 sample and reacting the bending moment. Having a pin in place of an externally located  
37 support allows for longitudinal support of the sample and means that the sample can be  
38 smoothly driven through the zero moment position. The principal of Saint-Venant means that  
39 these pins should provide a similar bending moment to a more traditional support assembly  
40 at distances far from the support.

41          The sample is of rectangular section in the bending region with a thickness of 5mm in  
42 the direction perpendicular to the plane of the neutral axis and 7mm wide. These dimensions  
43 have been optimized to balance the load and deflection needed from the mechanical bellows  
44 and minimize the temperature gradient in the sample whilst maintaining the space required to  
45 mount instrumentation.

1 The bending method has a large advantage over the tensile method in that the  
2 thermal and mechanical strains are decoupled from each other. In the standardized (tensile)  
3 method, the first part of the test is to determine the samples thermal expansion, the desired  
4 mechanical strain is then applied as a total strain which is corrected for the thermal  
5 expansion induced in the sample. In a bending test, the maximum mechanical strain is only  
6 applied far from the neutral bending axis but is independent of temperature (it is a function of  
7 geometry and force only). In addition to this the bending method allows for large stresses to  
8 be developed from relatively limited forces. However, it should be noted that any plasticity in  
9 the sample makes the relation between bending moment and stress much more difficult to  
10 understand and interpret than in a tensile sample.

11 The thermal expansion elongating the length between the reaction pins is estimated  
12 to change the bending moment by only 2%.

13 The mechanical loading of the device comes from a pressurized bellows. There are  
14 two bellows on each side of the sample. The bellows are pressurized to provide a force  
15 perpendicular to the sample.

16 The outer sleeve of the test device is utilized to react the bending moment and  
17 calculation has shown that this will induce a stress of around 30MPa in the structure. The  
18 paniers will be instrumented with a strain gauge, thermocouple and dosimeters.

## 19 **V.D. Temperature Control of Samples**

20 As discussed above, the contemporary techniques available for temperature control  
21 in MTRs are unsuitable for this device due to the large temperature fluctuation desired within  
22 a single cycle. The innovative part of this test device is the temperature control system  
23 whereby the thickness of gas gap between the samples and the test device is changed via  
24 the use of an edge-welded bellows. Prototyping of this device is foreseen in 2017/2018. With  
25 this technique, the device itself remains at around 85°C meaning that the bellows and  
26 associated brazed joints will also remain at around this temperature as only the samples  
27 achieve the high temperatures.

28 The arrangement proposed is shown in Figure 10. Calculation has shown that this  
29 should be able to adjust the temperature of a stainless steel sample from around 150°C to  
30 over 600°C with a gas gap of between 10µm and 350µm respectively (c.f. Figure 11). The  
31 calculation assumed a nuclear heat load of 15W/g and that the sample radiates heat to an  
32 enclosure at 40°C.

33 It should be noted that in a stainless steel sample, there is anticipated to be a thermal  
34 gradient of around 40°C. Although a thinner sample could alleviate this, the increased  
35 deformation during the mechanical strain application and its implications for the loading  
36 device mean that this is likely to be the optimum design (note the gradient will fall to ~15°C in  
37 the case of ferritic steels due to their higher thermal conductivity).

38 An estimation of the time taken for a temperature change to occur can be obtained by  
39 dividing the amount of energy stored to that transferred, as the helium gap is the limiting part  
40 of the transfer process it is assumed to be the sole thermal resistance. The pseudo heat  
41 transfer coefficient is estimated as the average thermal conductivity divided by the gap  
42 thickness. The time constant is estimated at around 30s, meaning that 85% of the  
43 temperature transition is achieved in 60s, 95% in 90s and 99.3% in 150s. This must be  
44 accounted for in the experimental thermal mechanical strain pattern and will limit the number  
45 of thermal cycles available in a calendar time.

## 1 VI. Conclusions

2 A collaborative project between CCFE in the UK and CEA in France has been started  
3 in order to design test devices for the JHR (Europe's newest MTR) which will help to close  
4 some of the present gaps in knowledge necessary in order to commercialize fusion  
5 technology.

6 Three test devices have been conceptually designed;

- 7 • A device intended to facilitate design of diagnostic windows, in addition to  
8 determining the optical properties during neutron irradiation, the mechanical  
9 stages allow for sub-critical crack growth testing (an important part of any  
10 structural justification for ceramic materials).
- 11 • A device intended to allow for testing at cryogenic temperatures of around  
12 50K. This device is intended to allow for testing of materials relevant to  
13 superconducting magnets, not simply the conducting elements but also any  
14 supporting structures. In addition to this the device could be used for  
15 validation and development of primary damage models in material.
- 16 • A device looking at thermo-mechanical fatigue, ranging between 150-600°C  
17 with a mechanical stress applied up to  $\pm 250$ MPa. This device should aid in  
18 reducing unnecessary conservatism arising from designing first-wall  
19 components using fatigue data based upon primary stresses only.

20 This project will continue in order to develop these designs further including prototyping of  
21 critical systems, nuclear and thermo-hydraulic calculations and structural design to relevant  
22 codes and standards in order that these tools can be used in future to aid the material  
23 science needs of the fusion community.

24

## 1 Acknowledgements

2 The authors would like to thank the following people for their thoughtful reviews' and  
3 helpful critique of the conceptual designs; Mike Gorely, Nanna Heiburg, Monica Jong and  
4 Natalia Luzginova of CCFE, Brad Wynne from the University of Sheffield, Laurent Briottet,  
5 François Millet and Ludovic Vincent of the CEA.

6 **Funding statement to be added.**

## 7 References

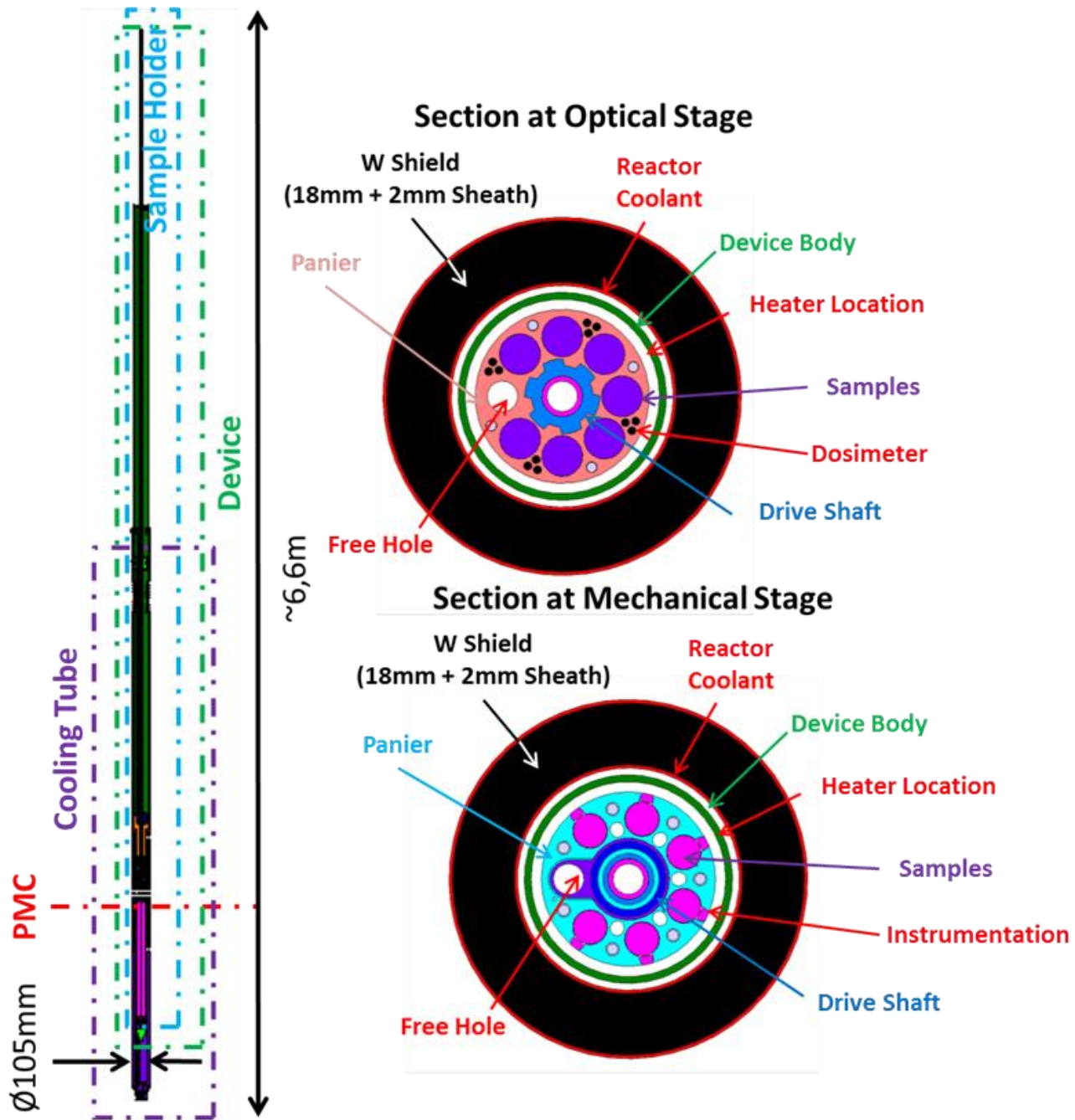
8

- [1] G. Bignan and J. Estrade, "The Jules Horowitz Reactor: A new High Performance European MTR (Material Testing Reactor) with Modern Experimental Capabilities: Toward an International User Facility," in *International Group on Research Reactors (IGORR)*, Daejeon, South Korea, 2013.
- [2] K. Ikeda, N. Holtkamp, M. Pick, F. Gauche, P. Garin, B. Bigot, J. Luciani, J. Mougnot, J. Watteau, B. Saoutic, A. Becoulet and P. B. B. Libeyre, "ITER, a major step toward nuclear fusion energy," *Revue Generale Nucleaire*, vol. 1, pp. 24-114, 2007.
- [3] G. Federici, R. Kemp, D. Ward, C. Bachmann, T. Franke, S. Gonzalez, C. Lowry, M. Gadomska, J. Harman, B. Meszaros, C. Morlock, F. Romanelli and R. Wenninger, "Overview of EU DEMO Design and R&D Activities," *Fusion Engineering and Design*, vol. 89, no. 7-8, pp. 882-889, 2014.
- [4] C. Colin, J. Pierre, C. Blandin, C. Gonner, M. Auclair and F. Rozenblum, "Test devices in Jules Horowitz Reactor dedicated to the material studies in support to current and future Nuclear Power Plants," in *Fontevraud 8 - Contribution of Materials Investigations and Operating Experience to LWRs' Safety, Performance and Reliability*, Avignon, France, 2014.
- [5] G. Hopkins and R. Price, "Fusion reactor design with ceramics," *Nuclear Engineering and Design. Fusion*, vol. 2, no. 1, pp. 111-143, 1985.
- [6] K. Breder and A. Wereszczak, "Fatigue and Slow Crack Growth," in *Craner, D and Richerson, D; Mechanical Testing Methodology for Ceramic Design and Reliability*, ISBN 0-8247-9567-9, Marcel Dekker, Inc, 1998, pp. 223-295.
- [7] C. Gormezano, "RF Systems for Heating and Current Drive in Fusion Experiments," JET-P(96)57, 1996.
- [8] T. Shikama, S. Zinkle, K. Shiiyama, L. Snead and E. Farnum, "Electrical properties of ceramics during reactor irradiation," *Journal of nuclear Materials*, Vols. 258-263, no. 2, pp. 1867-1872, 1998.
- [9] S. Zinkle and L. Mansur, "Radiation Effects in Materials, with emphasis on Insulators for Couplers," in *Workshop on High-Power Couplers for Superconducting Accelerators*, Jefferson Laboratory, 2002.
- [10] G. Pells et R. boothby, «The effects of gamma irradiation on subcritical crack growth in alumina,» *Journal of Nuclear Materials*, vol. 256, n° 11, pp. 25-34, 1998.
- [11] W. Creyke, I. Sainsbury and R. Morrell, *Design with non-ductile Materials*, London: Applied Science Publishers, 1982.
- [12] N. Casal, C. Vorpahl, R. Reichle, G. Vayakis, R. Barnsley and J. Barbero, "Functional Materials for ITER Diagnostics Systems - Radiation Aspects," in *3rd IAEA-ITER Technical Meeting*, Vienna, 2015.

- [13] T. Shikama, T. Kakuta, N. Shamoto, N. Minoru and T. Sagawa, "Behaviour of Developed Radiation-Resistant Silica-Core Optical Fibres under Fission Reactor Irradiation," *Fusion Engineering and Design*, Vols. 51-52, pp. 179-183, 2000.
- [14] AFNOR, NF EN 843-3, Céramiques Techniques Avancées, Propriétés Mécaniques des Céramiques Monolithiques à Température Ambiente: Partie 3 : Détermination des Paramètres de Propagation Sous-Critique des Fissures à Partir des Essais de Résistance à la Flexion Réalisés à Vitesse de Contrainte Constante, Norme Européenne, Norme Française.
- [15] W. Young et R. Budynas, Roark's Formulas for Stress and Strain 7th Ed, ISBN: 0-07-072542-X: McGraw-Hill, 2002.
- [16] OECD, OCDE/GD(95)81/PART5, Paris 1995, Megascience, the OECD forum.
- [17] F. Schmalz, F. Blom, S. Kamer et D. Ketema, «Design for in-pile thermal fatigue of first wall mock-ups under ITER relevant conditions,» *Fusion Engineering and Design*, vol. 82, pp. 1820-1824, 2007.
- [18] N. -. L. Phung, Fatigue sous tres faibles amplitudes de contrainte : Analyse de mecanismes precurseurs de l'amorçage de fissures dans le cuivre polycristallin, Ecole des Arts et Metiers, 2012.
- [19] A. Le Pécheur, Fatigue thermique d'un acier inoxydable austénitique : influence de l'etat de surface par une approche multi-echelles, Ecole Centrale Paris, 2008.

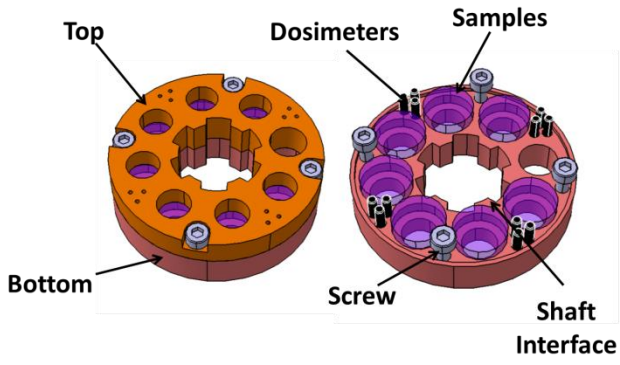
1  
2

1 Figures



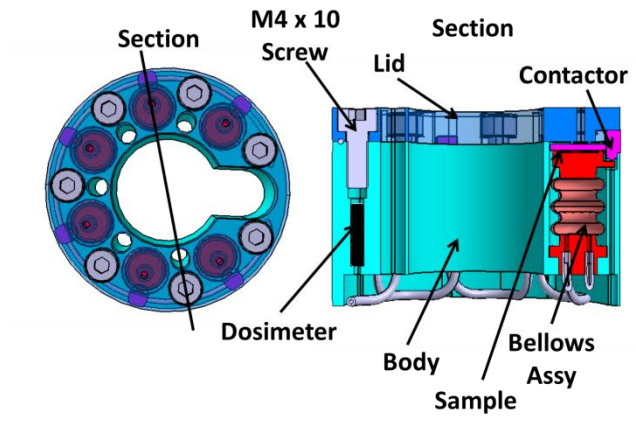
2  
3

Figure 1, overview of the ceramic functional material test device



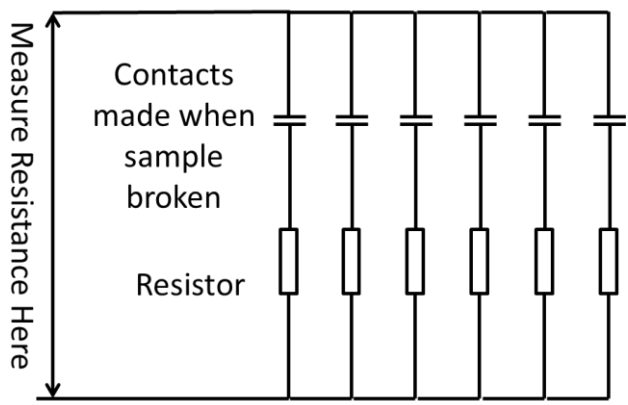
1  
2

Figure 2, paniers for optical samples



3  
4

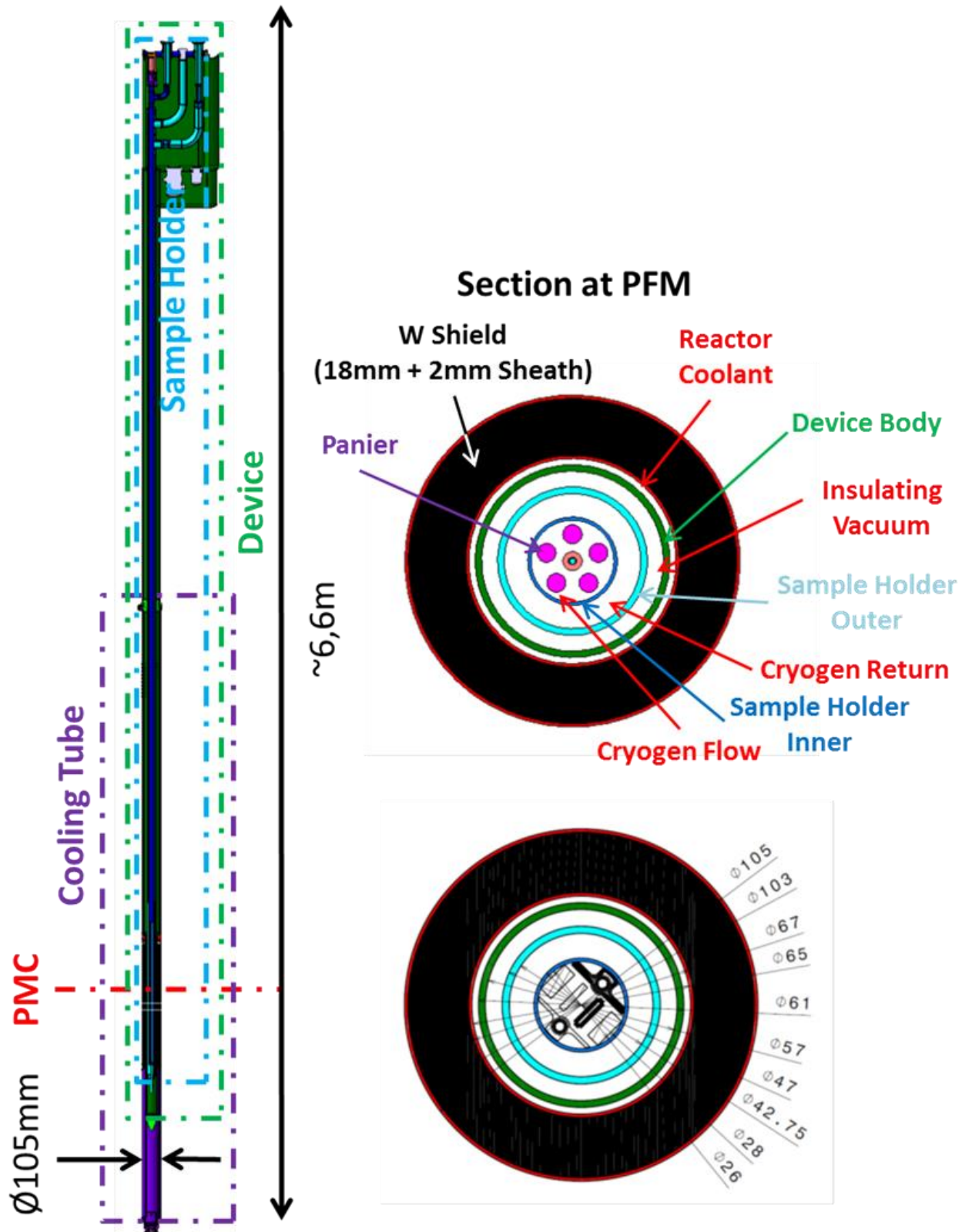
Figure 3, paniers for mechanical samples



5  
6

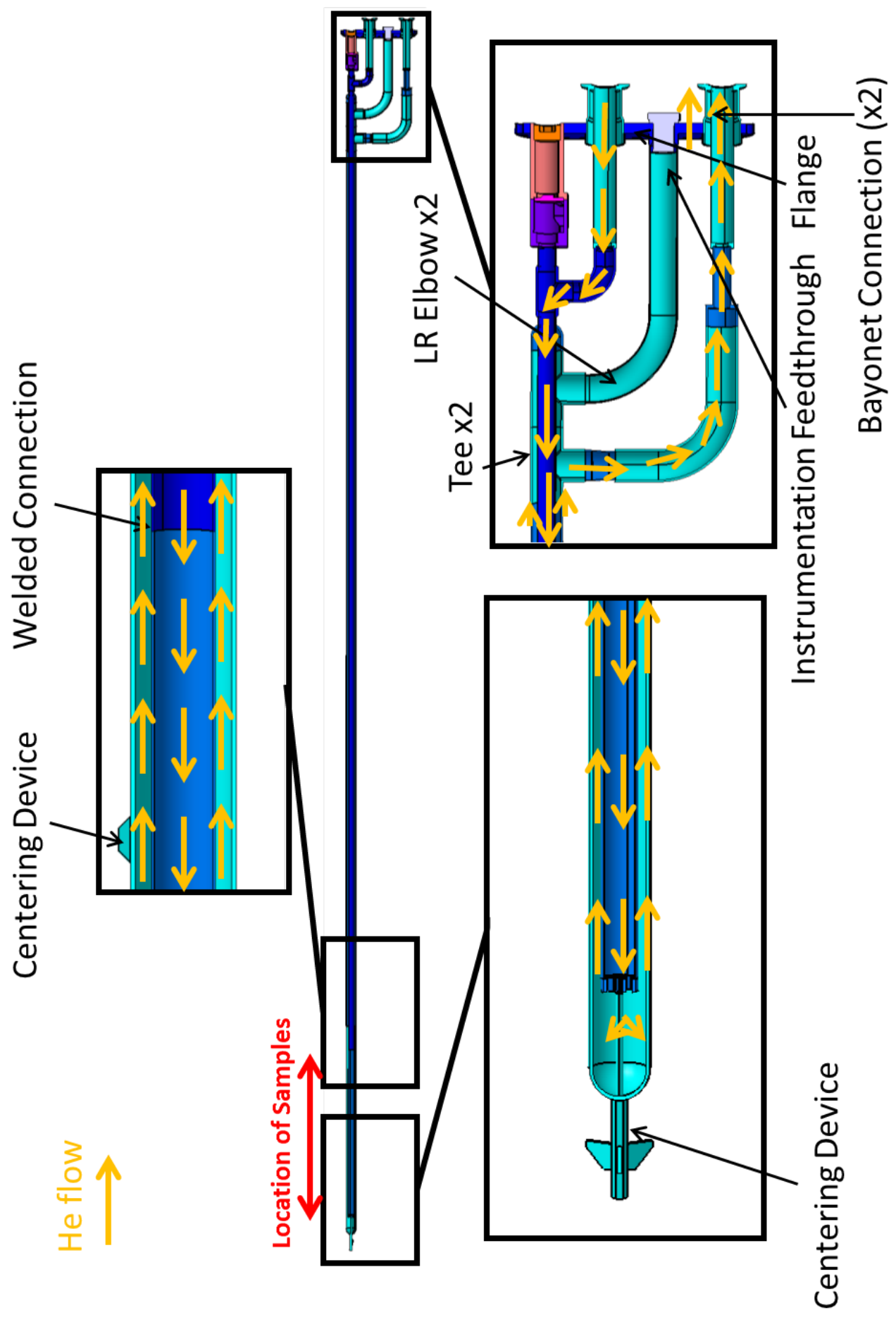
Figure 4, schematic for sample time to failure measurement system





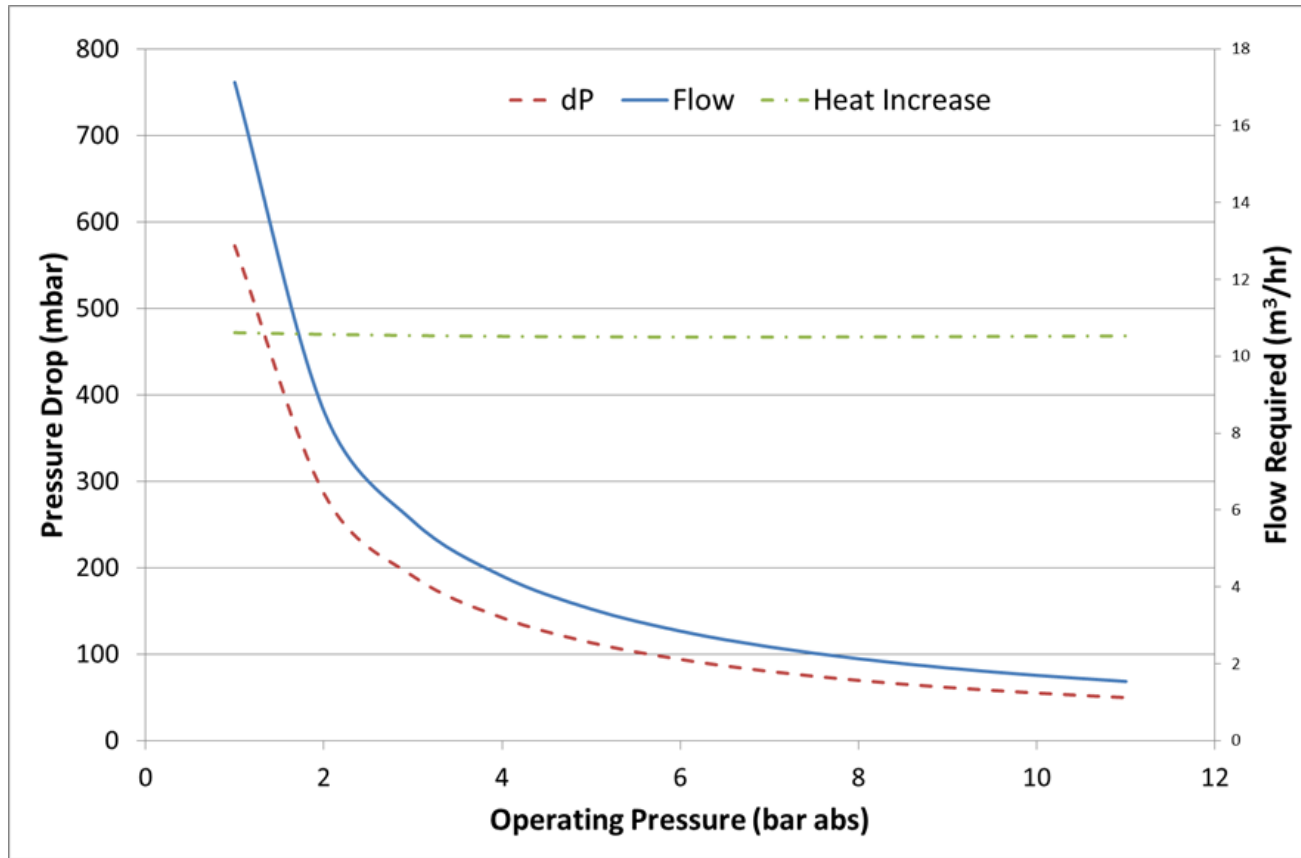
1  
2

Figure 5, overview of cryogenic test device



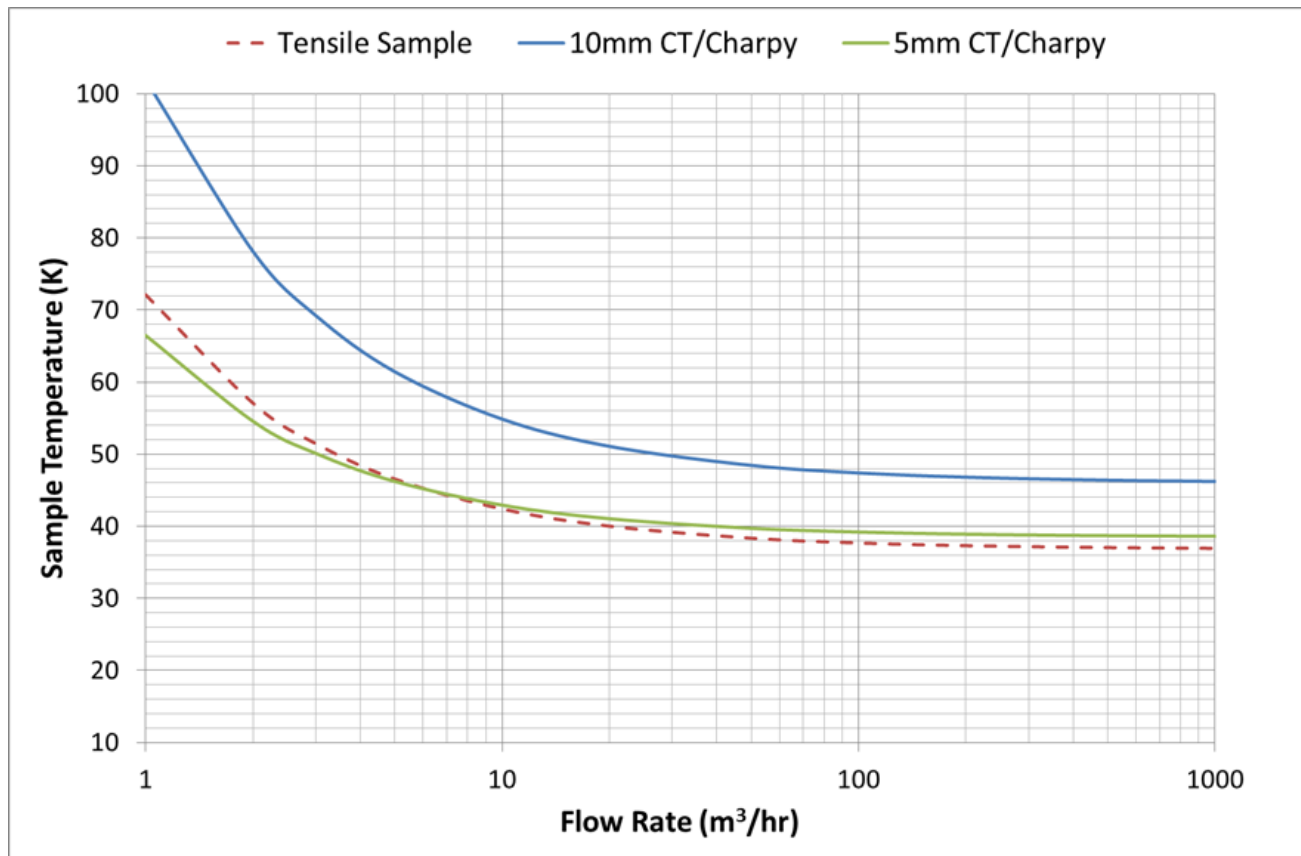
1  
2

Figure 6, overview of the sample holder for the cryogenic test device



3  
4

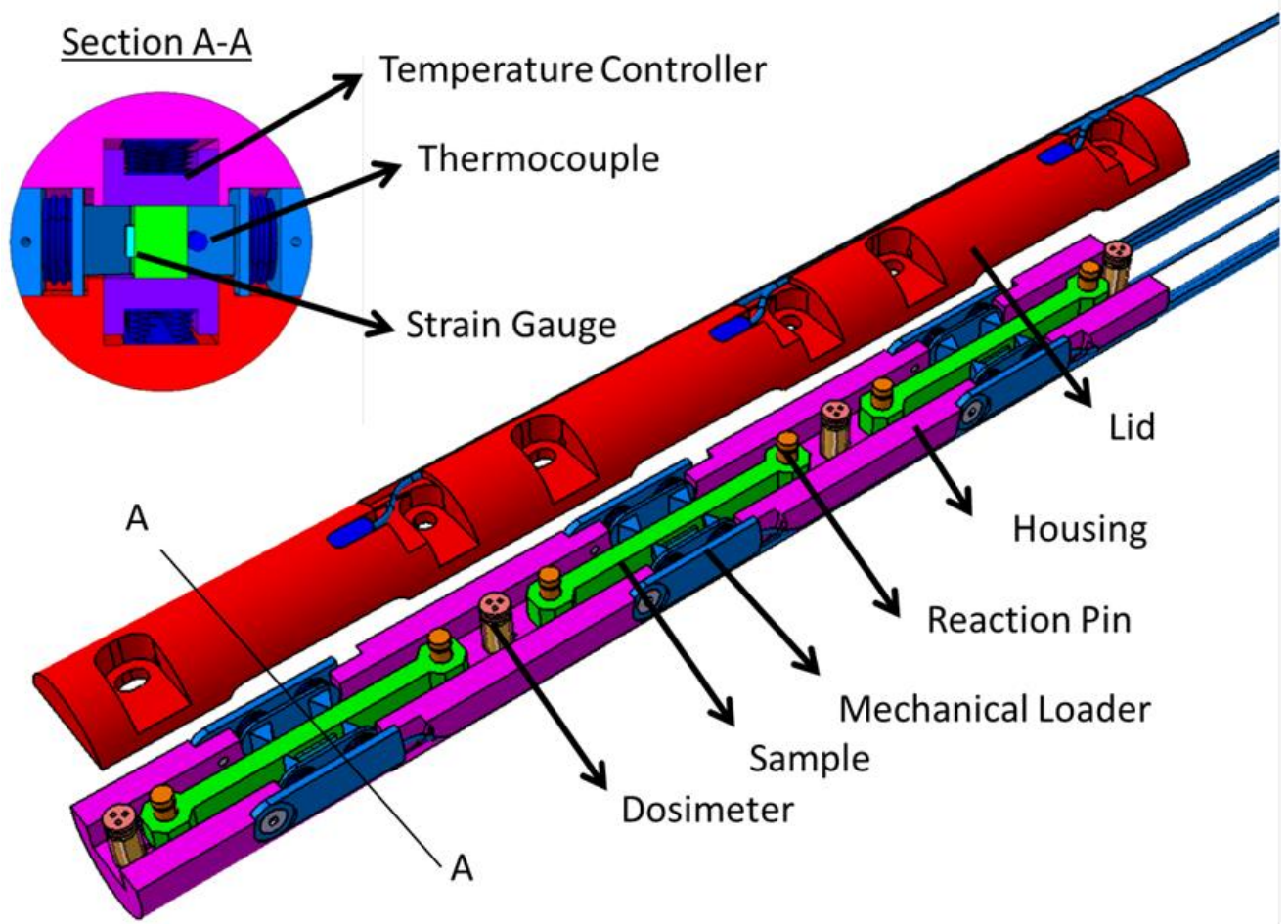
Figure 7, sensitivity analysis to cryogenic system pressure



5

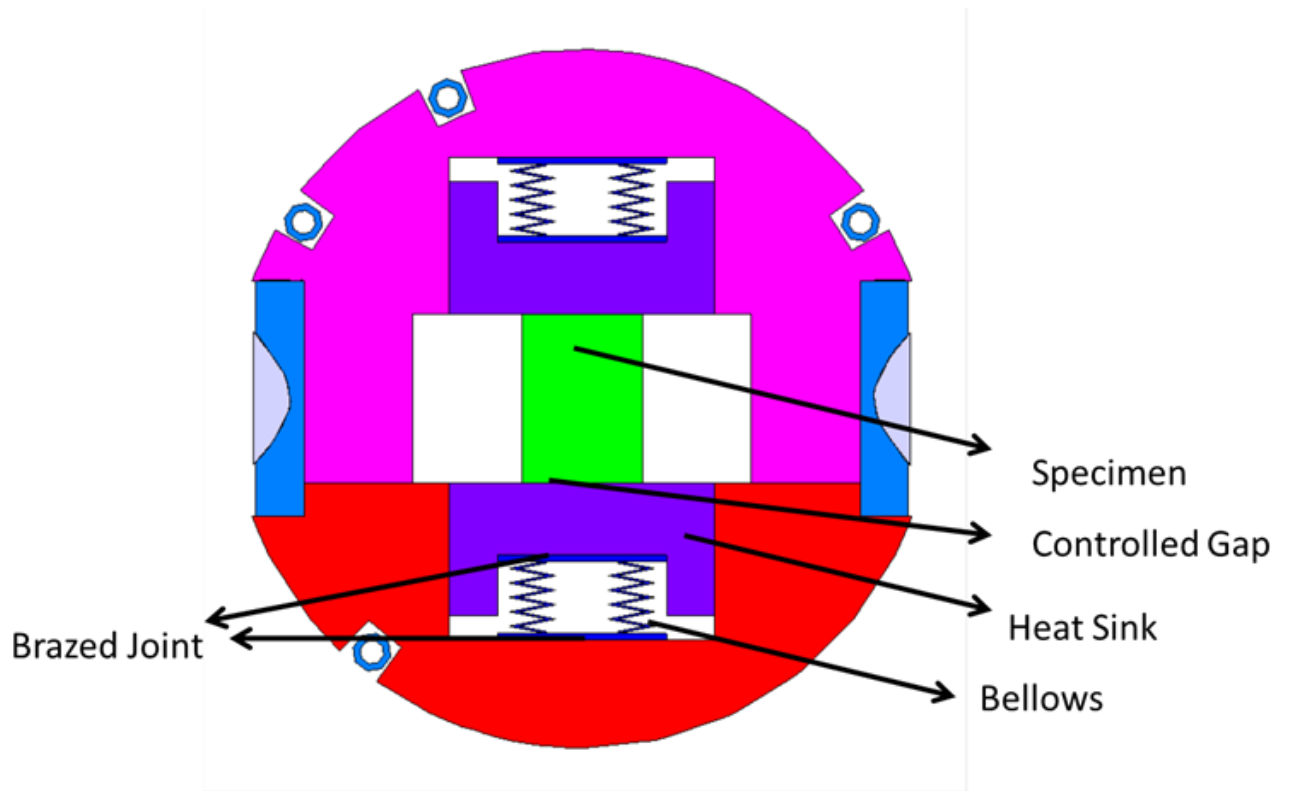
1

Figure 8, sensitivity of sample temperatures to cryogen flow



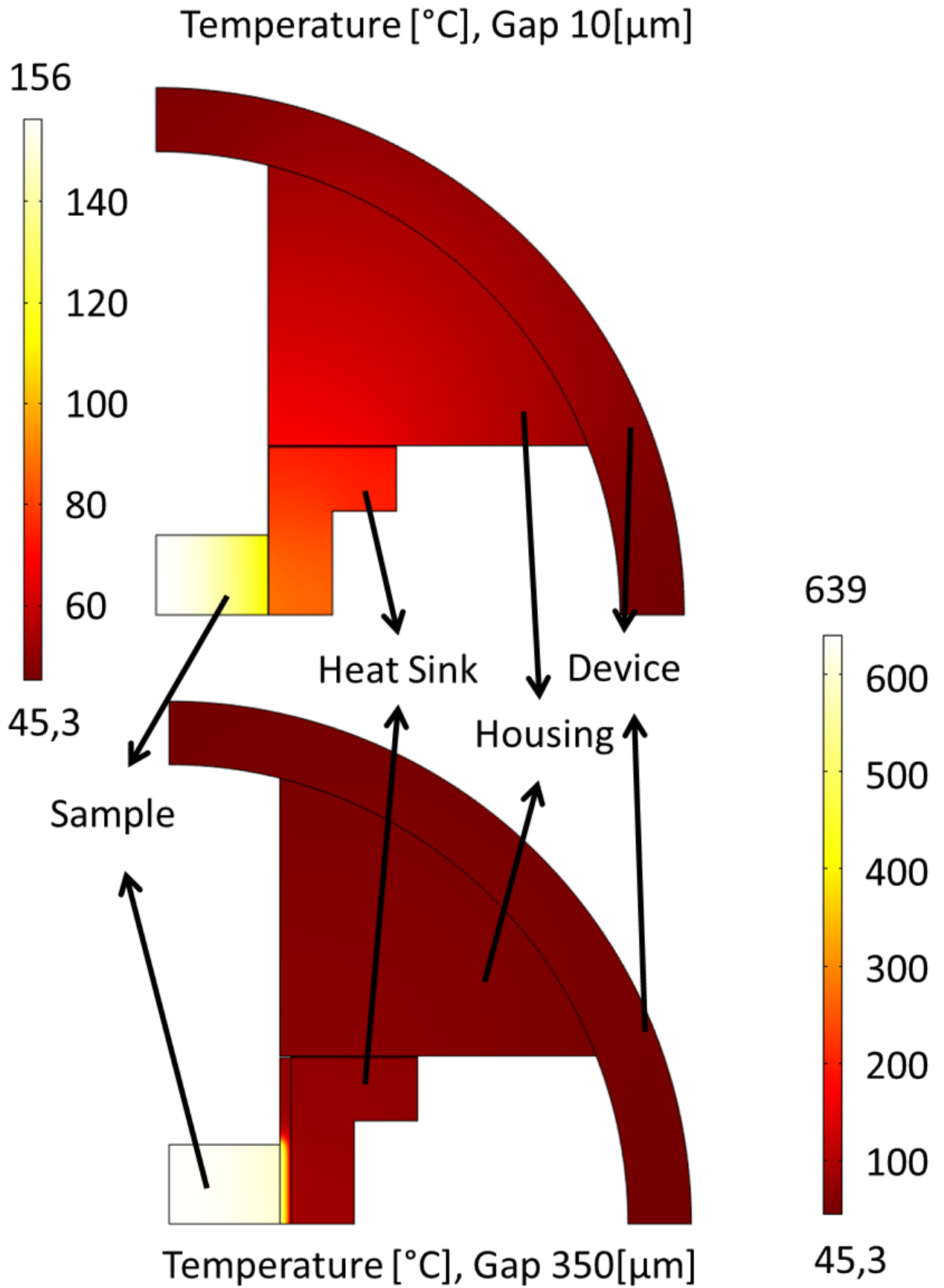
2  
3

Figure 9, overview of the thermo-mechanical fatigue test device



1  
2

Figure 10, temperature control system proposed for thermo-mechanical fatigue test device



1  
2

Figure 11, finite element results of modelling temperature control system